*Progress In Electromagnetics Research M, Vol. 46, 153–163, 2016*

# Mesh Optimization for Maxwell's Equations with Respect to Anisotropic Materials Using Geometric Algebra

**Mariusz Klimek[1, *], Sebastian Schöps[1, 2], and Thomas Weiland[2]**

**Abstract**—Clifford's Geometric Algebra provides an elegant formulation of Maxwell's equations in the space-time setting. Its clear geometric interpretation is used to derive a goal function, whose minimization results in Hodge-optimized material matrices being diagonal or diagonal-dominant. Effectively it is an optimization of the primal/dual mesh pair of a finite difference based discretization scheme taking into account the material properties. As a research example, a standing wave in 2D cavity filled with an anisotropic material is investigated. Convergence of the scheme for various choices of mesh pairs is discussed. The limitations of the method in the 3D case are presented.

## 1. INTRODUCTION

Clifford's Geometric Algebra (GA) in the context of discretization of Maxwell's equations is closely related to the Cell Method [3], Discrete Exterior Calculus [10] and to the Finite Integration Technique (FIT) [4]. All schemes are based on finite differences. For example, FIT allocates the electromagnetic quantities on points, edges, facets and three dimensional volumes of a primary and a dual grid such that they are natural discretization in terms of exterior algebra and differential forms. The time domain is typically treated afterward by the leap-frog scheme. On the other hand, the GA-based approach differs from that as it naturally performs discretization in space-time, i.e., taking immediately into account all four dimensions. Compared to the exterior algebra of differential forms GA gives more algebraic tools at the cost of explicit introduction of the metric. However, all approaches lead to practically equivalent schemes. This has been shown for the Cartesian grid case in [2].

The material relations link the quantities located at both, the primal and dual grid. In this paper we aim for grid conditions that allow to represent the relations as one-to-one connection of those quantities, i.e., one primal degree of freedom is linked to exactly a one dual. This is equivalent to diagonalizing the discrete Hodge star operator and yields eventually diagonal material matrices. The importance of this property comes from its impact on efficiency of the scheme: many matrix-vector multiplications and inversions of material matrices are carried out in the leap-frog time-integration of FIT-like schemes. This is obviously computationally more efficient and requires less data-storage if the matrices are diagonal. Attempts to achieve one-to-one properties via optimization of primal/dual mesh pairs in different context have been proposed, for example in [7]. However, in our case the Hodge star depends on material distributions which may be inhomogeneous, making it a function of space. Several formalisms have been proposed in related settings, for example anisotropic materials have been theoretically studied in [8] using classical tensor calculus, while differential forms have been used to recast Maxwell's equations in [9]. However, here GA was chosen due to its clearer geometric interpretation

*Received 4 November 2015, Accepted 4 February 2016, Scheduled 1 March 2016*

* Corresponding author: Mariusz Klimek (klimek@gsc.tu-darmstadt.de).

[1] Graduate School of Computational Engineering, Technische Universitaet Darmstadt, Dolivostrasse 15, Darmstadt D-64293, Germany. [2] Institut fuer Theorie Elektromagnetischer Felder, Technische Universitaet Darmstadt, Schlossgartenstrasse 8, Darmstadt D-64289, Germany.

compared to other formalisms. Nonetheless a translation of the results in terms of differential forms is straight forward.

The paper is structured as follows. In Section 2, GA is briefly outlined. The focus is on space-time algebra. For illustration, we present how complex numbers can be derived as a subalgebra in the 2D plane showing that GA may be perceived as a generalization of complex numbers to higher dimensional spaces. Section 3 is devoted to recasting Maxwell's equations in space time using space-time algebra. The integral form is preferred as it simplifies the derivation of the discretization. In Section 4, we discretize Maxwell's equations with special attention on material relations. The main result is a sufficient condition that guarantees diagonal material matrices. Section 5 is an application of the theory to the simple 2D problem. Comparison with existing approaches is performed. Section 6 shows the limitations of the method in 3D. In Section 7 the conclusions are drawn.

## 2. GEOMETRIC ALGEBRA OF MINKOWSKI SPACE-TIME

In GA, the fundamental operation is the *geometric product* of vectors, which is [1]

$$\begin{aligned} ab &\neq ba, && \text{(noncommutative)}\\ (ab)c &= a(bc), && \text{(associative)}\\ a(b+c) &= ab+ac, && \text{(left-distributive)}\\ (a+b)c &= ac+bc, && \text{(right-distributive)}\\ a^{-1} &= \frac{a}{a^2}, && \text{(invertible)} \end{aligned}$$

where $a$, $b$ and $c$ are vectors. A norm is defined through $|a|^2 := a^2 \in \mathbb{R}$. The geometric product of two vectors can be split into its symmetric (scalar) and antisymmetric (bivector) part

$$ab = \frac{1}{2}(ab+ba) + \frac{1}{2}(ab-ba) := a\cdot b + a\wedge b, \tag{1}$$

where $\cdot$ and $\wedge$ denote the *scalar* and *exterior* product. 4D Euclidean basis vectors are denoted by $\gamma_i$, $i \in \{x,y,z,t\}$, where $x$, $y$, $z$ are space coordinates, and $t$ is time. The convention is $\gamma_t^2 = +1$ and $\gamma_x^2 = \gamma_y^2 = \gamma_z^2 = -1$. Note that a vector is usually interpreted as an oriented 1D object. The *pseudoscalar* $I := \gamma_t\gamma_x\gamma_y\gamma_z$ gives a unique representation of any oriented 4D object ("space-time volume") $A_4$ through $A_4 = |A_4|I$. Its square is $I^2 = -1$. Relative 3D vectors $\sigma_k := \gamma_k\gamma_t$, $k = x,y,z$, square to $+1$ and are mutually orthogonal. Therefore, they are basis vectors of 3D space, but still (implicitly) contain temporal information. Additionally, $I = \sigma_x\sigma_y\sigma_z$ holds. We denote relative 3D vectors by, e.g.,

$$\vec{E} \equiv E^x\sigma_x + E^y\sigma_y + E^z\sigma_z. \tag{2}$$

The *geometric derivative* can be expressed as

$$\nabla = \gamma^\alpha\partial_\alpha = \gamma^t\partial_t + \gamma^x\partial_x + \gamma^y\partial_y + \gamma^z\partial_z = \gamma_t\partial_t - \gamma_x\partial_x - \gamma_y\partial_y - \gamma_z\partial_z, \tag{3}$$

where $\gamma^\alpha$ are reciprocal basis vectors, i.e., $\gamma^\alpha\cdot\gamma_\beta = \delta^\alpha_\beta$ where $\delta^\alpha_\beta$ denotes the Kronecker delta. Therefore, $\nabla$ is a vector from the algebraic perspective and an operator acting on the object on its right from operational point of view. The relative 3D geometric derivative takes a similar form

$$\vec{\nabla} = \sigma_i\partial_i = \sigma_x\partial_x + \sigma_y\partial_y + \sigma_z\partial_z. \tag{4}$$

For the comprehensive introduction of geometric calculus the reader is referred to [5].

### 2.1. Complex Numbers

For motivation, we show that complex numbers are a subalgebra of 2D GA. Suppose we are given a vector $r$ in the 2D plane. We **define** the real axis as $x$-coordinate line. The induced unit basis vectors are $e_x$ and $e_y$. Please note that we can define the real axis as any line in the plane, i.e., we can choose arbitrary unit vector instead of $e_x$. Then we identify the complex number $z$ associated with $r$ with

$$z = e_x r = e_x(xe_x + ye_y) = x + ye_xe_y = x + Iy. \tag{5}$$

First, we note that the 2D pseudoscalar $I := e_x e_y$ commutes with every complex number. Therefore, the algebra of complex numbers is commutative. Secondly, we see that its square is

$$I^2 = II = e_x e_y e_x e_y = -e_x e_x e_y e_y = -1. \tag{6}$$

Therefore, it is natural to identify $I$ with the imaginary unit. The complex conjugate of $z$ is $z^\dagger = re_x$. Suppose we are given a complex function $f = u(x,y)+Iv(x,y)$. Then we can state the Cauchy-Riemann equations as $\nabla f = 0$. We show it by expanding

$$\nabla f = (e_x\partial_x + e_y\partial_y)(u + Iv) = e_x(\partial_x u - \partial_y v) + e_y(\partial_y u + \partial_x v) = 0 \tag{7}$$

and noting that the equations in brackets are exactly the Cauchy-Riemann equations. Therefore, $\nabla f = 0$ holds for all analytic functions $f$. The result is less surprising if we multiply this condition by $e_x$ from the left and note that

$$e_x\nabla = e_x(e_x\partial_x + e_y\partial_y) = \partial_x + I\partial_y = \frac{\partial}{\partial x} - \frac{1}{I}\frac{\partial}{\partial y} = \frac{\partial}{\partial(x - Iy)} = \frac{\partial}{\partial z^\dagger} \tag{8}$$

Therefore, Eq. (7) is equivalent to more familiar property of analytic functions $\frac{\partial f}{\partial z^\dagger} = 0$, where in $f$ we changed the coordinates from $(x,y)$ to $z = x + Iy$ and $z^\dagger = x - Iy$. Operations on complex numbers have a clear geometric interpretation in the 2D plane and this remains a characteristic feature of GA in arbitrary dimensions.

## 3. MAXWELL'S EQUATIONS

The traditional form of Maxwell's equations separating space and time reads

$$\begin{cases} \vec{\nabla}\times\vec{E} = -\partial_t\vec{B} \\ \vec{\nabla}\cdot\vec{B} = 0 \end{cases} \quad \begin{cases} \vec{\nabla}\times\vec{H} = \partial_t\vec{D} + \vec{J} \\ \vec{\nabla}\cdot\vec{D} = \rho, \end{cases} \tag{9}$$

where $\rho$, $\vec{J}$, $\vec{E}$, $\vec{H}$, $\vec{D}$ and $\vec{B}$ are the electric charge density, electric current density, electric and magnetic field strengths, electric and magnetic field fluxes, respectively. Since Maxwell's equations are Lorentz invariant, we express them explicitly in space-time [1]

$$\nabla \wedge F = 0 \qquad \nabla \cdot G = J, \tag{10}$$

where $F := \vec{E} + I\vec{B}$, $G := \vec{D} + I\vec{H}$ and $J := (\rho + \vec{J})\gamma_0$. $\gamma_0$ is the four-velocity of the medium. If the medium is at rest, then $\gamma_0 = \gamma_t$. To derive the space-time form of Maxwell's integral equations we follow Hestenes [6]. We integrate (10) over an arbitrary bounded 3D star domain $\Omega \subset \Xi$, $\Xi$ being 4D space-time, and apply the fundamental theorem of geometric calculus [5, 6]. The obtained equations are coordinate-free, do not involve any differentiation and are ready to be applied to an arbitrary 3D space-time element:

$$\oint_{\partial\Omega} \left(d^2x\right)\cdot F = 0 \quad \text{and} \quad \oint_{\partial\Omega} \left(d^2x\right)\wedge G = \int_{\Omega} (d^3x)\wedge J. \tag{11}$$

Both Equations (11) are linked by material equations given by

$$\vec{D} = \mathcal{D}\left(\vec{E},\vec{B}\right) \quad \text{and} \quad \vec{H} = \mathcal{H}\left(\vec{E},\vec{B}\right). \tag{12}$$

Ohm's law is disregarded in this article. The *material mapping* $\xi$ is implicitly defined by

$$G = \mathcal{D}\left(\vec{E},\vec{B}\right) + I\mathcal{H}\left(\vec{E},\vec{B}\right) = \xi(F), \tag{13}$$

where $\vec{E} = \frac{1}{2}(F - \gamma_0 F\gamma_0)$ and $\vec{B} = \frac{1}{2I}(F + \gamma_0 F\gamma_0)$. We want to stress that the introduction of $\xi$ is not a complication of the material equations but a translation to the space-time algebra in a consistent manner.

For example, if the medium is isotropic, i.e., permittivity $\varepsilon$ and reluctance $\nu$ are scalars in

$$\mathcal{D}\left(\vec{E},\vec{B}\right) = \varepsilon\vec{E} \quad \text{and} \quad \mathcal{H}\left(\vec{E},\vec{B}\right) = \nu\vec{B} \tag{14}$$

we can directly calculate $G$ in terms of $F$ in the coordinate frame of the medium

$$G = \vec{D} + I\vec{H} = \varepsilon\vec{E} + \nu I\vec{B} = \varepsilon\frac{1}{2}\left(F - \gamma_0 F\gamma_0\right) + \nu\frac{1}{2}\left(F + \gamma_0 F\gamma_0\right) = \frac{1}{2}\left[(\varepsilon+\nu)F - (\varepsilon-\nu)\gamma_0 F\gamma_0\right], \quad (15)$$

therefore we obtain a simple coordinate-free form of $\xi$ for isotropic media

$$\xi(X) = \frac{1}{2}\left[(\varepsilon+\nu)X - (\varepsilon-\nu)\gamma_0 X\gamma_0\right]. \quad (16)$$

However, in this paper we are interested in more complex case of symmetric anisotropic media, i.e.,

$$\mathcal{D}\left(\vec{E},\vec{B}\right) = (\sigma_x,\sigma_y,\sigma_z)\begin{pmatrix} \varepsilon_{xx} & \varepsilon_{xy} & \varepsilon_{xz} \\ \varepsilon_{xy} & \varepsilon_{yy} & \varepsilon_{yz} \\ \varepsilon_{xz} & \varepsilon_{yz} & \varepsilon_{zz} \end{pmatrix}\begin{pmatrix} E^x \\ E^y \\ E^z \end{pmatrix} \quad (17)$$

and

$$\mathcal{H}\left(\vec{E},\vec{B}\right) = (\sigma_x,\sigma_y,\sigma_z)\begin{pmatrix} \nu_{xx} & \nu_{xy} & \nu_{xz} \\ \nu_{xy} & \nu_{yy} & \nu_{yz} \\ \nu_{xz} & \nu_{yz} & \nu_{zz} \end{pmatrix}\begin{pmatrix} B^x \\ B^y \\ B^z \end{pmatrix}. \quad (18)$$

In this case using the explicit definition of $\xi$ obtained by inserting (17) and (18) into (13) one can verify that

$$\xi(B_1)\cdot B_2 = B_1\cdot\xi(B_2) \quad (19)$$

holds for all bivectors $B_1$ and $B_2$. Therefore, the material mapping is self-conjugate. Instead of presenting a general expression for $\xi$ we rather present a few important special cases. Since $\xi$ is linear, to evaluate for arbitrary $F$

$$\xi(F) = \xi(\vec{E}) + \xi(I\vec{B}) = E^i\xi(\sigma_i) + B^i\xi(I\sigma_i) \quad (20)$$

it is sufficient to know

$$\xi(\sigma_i) = \varepsilon_{ij}\sigma_j \quad \text{and} \quad \xi(I\sigma_i) = \nu_{ij}I\sigma_j. \quad (21)$$

For the inverse $\xi^{-1}$ the interesting equations are

$$\xi^{-1}(\sigma_i) = \left[\varepsilon^{-1}\right]_{ij}\sigma_j \quad \text{and} \quad \xi^{-1}(I\sigma_i) = \mu_{ij}I\sigma_j, \quad (22)$$

where permeability $\mu = \nu^{-1}$.

## 4. DISCRETE SETTING

We discretize the 4D spacetime domain $\Xi$ into a set of primal cells $\Xi_i$. The boundary of each primal cell consists of 3D volumes $\Omega_k$ and the boundary of each $\Omega_k$ consists of 2D facets $\Delta_j$. We define edges and points in a similar manner. The structure above is referred as the *primal mesh*. A second, *dual mesh* is introduced in a similar fashion. Dual cells, dual volumes and dual facets are denoted by $\widetilde{\Xi}_i$, $\widetilde{\Omega}_k$ and $\widetilde{\Delta}_j$, respectively. The meshes are constructed in such a way that each $\Xi_i$ contains exactly one dual node, each $\Omega_k$ intersects one dual edge, each $\Delta_j$ intersects one $\widetilde{\Delta}_j$, etc.

A discrete version of Maxwell's equations "Maxwell's 4D grid equations" is obtained by applying the left equation of Eq. (11) to each primal volume, and the right one on Eq. (11) to each dual volume:

$$\oint_{\partial\Omega_k}\left(d^2x\right)\cdot F = 0 \quad \text{and} \quad \oint_{\partial\widetilde{\Omega}_k}\left(d^2x\right)\wedge G = \int_{\widetilde{\Omega}_k}\left(d^3x\right)\wedge J. \quad (23)$$

These integrals are sums of integrals of the type

$$f_j := \int_{\Delta_j}\left(d^2x\right)\cdot F \quad \text{and} \quad g_j := I^{-1}\int_{\widetilde{\Delta}_j}\left(d^2x\right)\wedge G, \quad (24)$$

which we define as **scalar** degrees of freedom (DoF) on the primal and dual mesh respectively. The approximate fields $F_j^*$ described by degrees of freedom follows from

$$f_j = \int\limits_{\Delta_j} \left(d^2x\right) \cdot F \approx \left[\int\limits_{\Delta_j} \left(d^2x\right)\right] \cdot F_j = W_j \cdot F_j = W_j F_j^*, \tag{25}$$

where $F_j$ is the field $F(x_j)$ at some point $x_j \in \Delta_j$ (typically the center), $W_j$ is the bivector representing the magnitude and the mean orientation of the facet $\Delta_j$

$$W_j := \int\limits_{\Delta_j} \left(d^2x\right) \tag{26}$$

and $F_j^*$ is defined such that the last equality in Eq. (25) holds

$$F_j^* := W_j^{-1}(W_j \cdot F_j), \tag{27}$$

i.e., it is the projection of $F_j$ onto the primal facet. The approximate field $F_j$ is thus decomposed into the part $F_j^*$ stored in the degree of freedom $f_j$ and the part $F_j^0$ not stored at $\Delta_j$

$$F_j = F_j^* + F_j^0. \tag{28}$$

Performing similar manipulations on the dual mesh we are lead to

$$Ig_j \approx \widetilde{W}_j G_j^* \tag{29}$$

and the analogous decomposition into stored and not-stored fields

$$G_j = G_j^* + G_j^0, \tag{30}$$

where

$$\widetilde{W}_j := \int\limits_{\widetilde{\Delta}_j} \left(d^2x\right), \quad G_j^* := \widetilde{W}_j^{-1}\left(\widetilde{W}_j \wedge G_j\right) \quad \text{and} \quad G_j := G(x_j), \quad x_j \in \widetilde{\Delta}_j. \tag{31}$$

To illustrate the steps made above, we consider a special case when $\Delta_j$ is a rectangle in $(t,\, z)$ plane: $\Delta_j = [t_1, t_2] \times [z_1, z_2]$. We note that the DoF

$$f_j = \int\limits_{\Delta_j} \left(d^2x\right) \cdot F = \int\limits_{t_1}^{t_2} dt \int\limits_{z_1}^{z_2} dz \gamma_z \gamma_t \cdot F = \int\limits_{t_1}^{t_2} dt \int\limits_{z_1}^{z_2} dz E^z \tag{32}$$

is related only to the $z$ component of the electric field $E^z$. The bivector representing the rectangle is simply calculated

$$W_j = \int\limits_{\Delta_j} \left(d^2x\right) = \int\limits_{t_1}^{t_2} dt \int\limits_{z_1}^{z_2} \gamma_z \gamma_t = \Delta z \Delta t \gamma_z \gamma_t = \Delta z \Delta t \sigma_z. \tag{33}$$

The approximate field $F_j = \vec{E}(x_j) + I\vec{B}(x_j)$, where $x_j \in \Delta_j$. The stored component of the approximate field is

$$F_j^* = W_j^{-1}\left(W_j \cdot F_j\right) = \frac{\sigma_z}{\Delta z \Delta t}\left(\Delta z \Delta t \sigma_z \cdot F_j\right) = E^z(x_j)\sigma_z, \tag{34}$$

while the non-stored component is

$$F_j^0 = E^x(x_j)\sigma_x + E^y(x_j)\sigma_y + I\vec{B}(x_j). \tag{35}$$

From (25) we obtain $F_j^* \approx f_j / W_j$, which for the rectangle considered reads

$$E^z(x_j)\sigma_z \approx \frac{1}{\Delta z \Delta t} \int\limits_{t_1}^{t_2} dt \int\limits_{z_1}^{z_2} dz E^z \sigma_z = \frac{f_j}{\Delta z \Delta t} \sigma_z, \tag{36}$$

where the exact error depends on the location of $x_j \in \Delta_j$. We have seen that $f_j$ is the DoF related to $E^z$. In classical discretization schemes, e.g., FIT [4], one would rather introduce the line-integrated quantity

$$\widehat{e}_j(t) = \int_{z_1}^{z_2} dz E^z \tag{37}$$

as the DoF associated with $E^z$, which is related to the 4D DoF

$$f_j = \int_{t_1}^{t_2} dt \widehat{e}_j(t). \tag{38}$$

### 4.1. Material Mapping

In the continuous setting the material mapping $\xi$ (13) relates the fields $F$ and $G$, which we afterward discretize on primal and dual meshes, respectively. Therefore, its discrete equivalent will link $\{f_j\}$ and $\{g_j\}$ and can be used, e.g., to express $\{g_j\}$ in terms of $\{f_j\}$. However, while Maxwell's grid equations are approximation-free, the discretization of material equations will introduce an error. The discrete material mapping reads

$$Ig_j \approx \widetilde{W}_j \wedge G_j = \widetilde{W}_j \wedge \overline{\xi}_j(F_j) = \widetilde{W}_j \wedge \overline{\xi}_j(F_j^*) + \widetilde{W}_j \wedge \overline{\xi}_j(F_j^0), \tag{39}$$

where $\overline{\xi}_j$ is $\xi$ averaged over $\widetilde{\Delta}_j$, i.e.,

$$\overline{\xi}_j(B) := \left|\widetilde{W}_j\right|^{-1} \int_{\widetilde{\Delta}_j} |d^2x| \xi(B), \quad \forall B = \text{const.} \tag{40}$$

We note that if we represent $\xi$ as a matrix with entries $\xi_{\alpha\beta} = \xi(\gamma_\alpha \wedge \gamma_\beta)$, then $\overline{\xi}_{j,\alpha\beta}$ is an average of $\xi_{\alpha\beta}$, i.e., we can average each entry independently. Since only $F_j^*$ is stored in $f_j$ and $F_j^0$ not, in order to obtain one-to-one relation between $f_j$ and $g_j$

$$\widetilde{W}_j \wedge \overline{\xi}_j(F_j^0) = \widetilde{W}_j \wedge \overline{\xi}_j\left(\underline{W}_j\right) |F_j^0| = 0 \tag{41}$$

must hold, and therefore

$$\widetilde{W}_j \wedge \overline{\xi}_j\left(\underline{W}_j\right) = 0, \tag{42}$$

since the magnitude of non-stored field $|F_j^0|$ is in general not zero. Above, we have assumed $\xi$ to be linear and introduced $\underline{W}_j$, which is an arbitrary bivector satisfying $\underline{W}_j \cdot W_j = 0$. Moreover we note that the following condition depends only on the materials involved and facets of the mesh pair

$$\widetilde{W}_j \wedge \overline{\xi}_j\left(\underline{W}_j\right) = \left(I\widetilde{W}_j\right) \cdot \overline{\xi}_j\left(\underline{W}_j\right) = \overline{\xi}_j^\dagger\left(I\widetilde{W}_j\right) \cdot \underline{W}_j = 0, \tag{43}$$

where $\overline{\xi}_j^\dagger$ is the conjugate of $\overline{\xi}_j$. The conjugate is defined such that for all bivectors $B_1$, $B_2$ it holds

$$\overline{\xi}_j^\dagger(B_1) \cdot B_2 = B_1 \cdot \overline{\xi}_j(B_2) \tag{44}$$

and it coincides with the conjugate in the traditional linear algebra sense. Therefore, the condition for one-to-one correspondence reads

$$\underline{W}_j \cdot W_j = 0 \Rightarrow \overline{\xi}_j^\dagger\left(I\widetilde{W}_j\right) \cdot \underline{W}_j = 0 \tag{45}$$

for all $\underline{W}_j$ and is implied by

$$W_j \cdot \underline{W}_j = 0 \quad \text{and} \quad \overline{\xi}_j^\dagger\left(I\widetilde{W}_j\right) \cdot \underline{W}_j = 0, \tag{46}$$

which can be further simplified (by subtracting both equations) to

$$\left(\alpha W_j - \overline{\xi}_j^{\dagger}\left(I\widetilde{W}_j\right)\right)\cdot \underline{W}_j = 0 \qquad \forall \underline{W}_j, \tag{47}$$

where $\alpha \in \mathbb{R}$ is some scalar. Using the orthogonality property for non-degenerate inner products, we arrive at

$$\alpha W_j = \overline{\xi}_j^{\dagger}\left(I\widetilde{W}_j\right). \tag{48}$$

### 4.2. Cartesian Barycentric Grid

Let us consider the important special case of a Cartesian barycentric mesh, which is typically used for FIT-like schemes. We present the 4D space-time case, however, 3D and 2D grids are constructed analogously.

The nodes of the primal mesh are introduced as

$$r^p_{i,j,k,l} := (i\Delta t, j\Delta x, k\Delta y, l\Delta z), \tag{49}$$

where $i$, $j$, $k$, $l$ are integers. We further introduce edges, e.g., in $x$-direction we obtain

$$l^p_{i,j+1/2,k,l} := i\Delta t \times [j\Delta x, (j+1)\Delta x] \times k\Delta y \times l\Delta z, \tag{50}$$

that are oriented by the vector $\gamma_x$ in $x$-direction. For simplicity we omit the respective definitions for the other coordinate directions. Facets are given by

$$a^p_{i,j,k+1/2,l+1/2} := i\Delta t \times j\Delta x \times [k\Delta y, (k+1)\Delta y] \times [l\Delta z, (l+1)\Delta z], \tag{51}$$

with orientation defined by the bivector $\gamma_y\gamma_z$. Volumes in 3D and space-time volumes are defined in a similar way. The midpoint of any space-time volume, is identified with a point on the dual grid. We then proceed as explained above to obtain edges, facets, volumes and space-time volumes on the dual grid respectively [2].

### 4.3. Material Matrices

The discrete material mapping enables us to express $\{g_j\}$ in terms of $\{f_j\}$. If we arrange $\{g_j\}$ and $\{f_j\}$ into column vector $g$ and $f$, this can be written in the case of linear materials as

$$g = Mf, \tag{52}$$

where $M$ is called material matrix. In general, and the matrix $M$ is not diagonal; however, if Eq. (48) holds, then it is diagonal with entries

$$[M]_{jj} = I^{-1}\widetilde{W}_j \wedge \overline{\xi}_j\left(W_j^{-1}\right). \tag{53}$$

Now we will point out why the orthogonal dual mesh does not guarantee diagonal material matrices for anisotropic material. Suppose $\widetilde{\Delta}_j$ is a purely spatial facet, i.e., $\widetilde{W}_j \cdot \gamma_t = 0$. Then the DoF associated with $\widetilde{\Delta}_j$ is related to the electric flux $\vec{D}$ only:

$$\widehat{\widetilde{d}}_j = \int\limits_{\widetilde{\Delta}_j} dS\vec{n}\cdot\vec{D} = \int\limits_{\widetilde{\Delta}_j} dS\vec{n}\cdot\varepsilon(\vec{E}) \approx \vec{n}\cdot\overline{\varepsilon}(\vec{p})\widehat{e}_j + \vec{n}\cdot\overline{\varepsilon}(\vec{q})\widehat{e}^0_j, \tag{54}$$

where $\vec{p}$ is a unit vector along primal edge, $\vec{n}$ a unit vector normal to the dual facet $\widetilde{\Delta}_j$, and $\vec{q}$ the unit vector normal to $\vec{p}$, i.e., $\vec{p}\cdot\vec{q} = 0$. $\widehat{e}^0_j$ is the non-stored component of the field, which has to be interpolated using the DoFs stored at neighboring edges $\widehat{e}^0_j = \theta_j(\{\widehat{e}_{k\neq j}\})$, thus leading to non-diagonal entries in $M$. We see that non-diagonal entries will vanish if $\vec{n}\cdot\overline{\varepsilon}(\vec{q}) = 0$. Noting that in orthogonal grid $\vec{n} = \vec{p}$, we see that for $\vec{p}\cdot\vec{q} = 0$

$$\vec{p}\cdot\overline{\varepsilon}\,(\vec{q}) \tag{55}$$

is in general not zero, since $\overline{\varepsilon}$ will change the direction of $\vec{q}$. However, if $\vec{q}$ is the main axis of the $\overline{\varepsilon}$, then its direction will not be changed

$$\vec{p}\cdot\overline{\varepsilon}\,(\vec{q}) = \varepsilon_{qq}\vec{p}\cdot\vec{q} = 0, \tag{56}$$

thus $M$ is diagonal in this special case.

## 5. NUMERICAL EXAMPLE IN 2D

A standing wave in a square cavity is reduced to 2D by assuming $E^z = B^x = B^y = 0$. The wavelength is equal to the dimension of the cavity. The time interval of the simulation is $T = [0, t_{\max}]$, where $t_{\max}$ is equal to five periods of the wave. The permittivity tensor is assumed to be diagonal $\varepsilon = \mathrm{Diag}(\varepsilon_x, \varepsilon_y)$.

The Cartesian barycentric grid as depicted in Fig. 1(a) is well-suited for this exemplary problem. However, in traditional FIT the skew edges of a deformed grid, Fig. 1(b), lead to non-diagonal entries in the material matrix as explained in Section 4.3. Disregarding these entries endangers stability and convergence of the scheme. The red line in Fig. 1(d) shows that the numerical solution does not converge to the exact one in the case of orthogonal dual, where non-diagonal entries in $M$ have been neglected. In our proposed approach, where the dual mesh is adapted to the material property, the convergence of the scheme is conserved, while keeping material matrices diagonal, as can be seen from the green line in Fig. 1(d). For comparison, the convergence of the traditional 2D FIT is plotted with blue line.

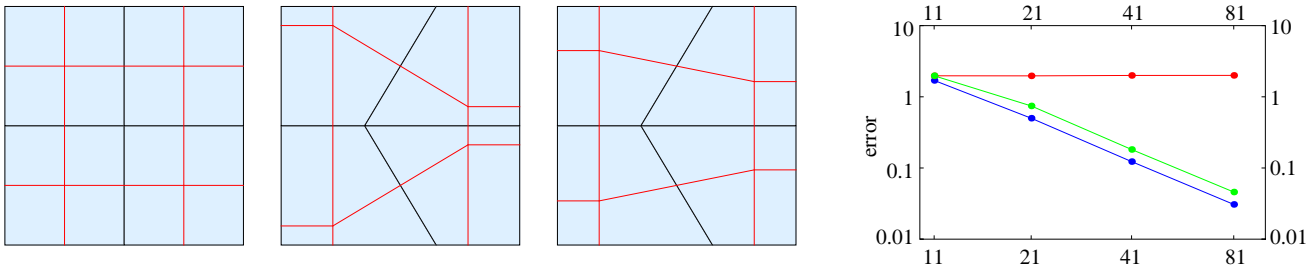


(a) Classical orthogonal Cartesian mesh

(b) Deformed orthogonal mesh, not optimized

(c) Deformed optimal mesh (for $\varepsilon_x/\varepsilon_y = 3$)

(d) Convergence plot

**Figure 1.** From left to right: conversion plots for (a) classical orthogonal FIT, (b) deformed orthogonal, (c) optimal (for $\varepsilon_x/\varepsilon_y = 3$) mesh pairs. Black and red lines represent primal and dual mesh, respectively. Figure (d) shows the convergence plot for $\varepsilon = \mathrm{Diag}(100, 1)$ and diagonal material matrices: Cartesian mesh (blue), deformed orthogonal (red) and deformed optimal (green). The error is defined as the relative error with respect to the analytic reference solution.

In 2D case the condition in Eq. (48) reduces to

$$\vec{p}_j = \alpha \overline{\varepsilon}_j(\vec{n}_j), \tag{57}$$

where $\vec{p}_j$ is a vector representing a primal edge and $\vec{n}_j$ is a vector normal (in Euclidean sense) to the dual edge. An exemplary mesh pair satisfying this condition is found analytically as depicted in Fig. 1(c).

Let us define the simulation error as a relative error of the line integrated electric field strength in the discrete $\ell^2$ vector norm and $\ell^\infty$ in time with respect to the analytic reference solution

$$\text{error} := \max_{t\in T} |\widehat{e} - \widehat{e}_a|_2 \,/\, \max_{t\in T} |\widehat{e}_a|_2 \,, \tag{58}$$

where $\widehat{e}$, see Eq. (38), is a vector composed of electric degrees of freedom at time $t = i\Delta t$, i.e.,

$$f_{j+in_e} = \int_{(i-1/2)\Delta t}^{(i+1/2)\Delta t} \widehat{e}_j(t)dt, \tag{59}$$

$n_e$ is number of edges, $\widehat{e}_a$ is calculated from the exact solution and $|\cdot|_2$ is the $\ell^2$-norm.

We have considered the example where $\varepsilon = \text{const.}$ because in this case the exact solution is known and traditional FIT approach works well. This made comparison of numerical solutions transparent. However, the idea of mesh optimization is by no means restricted to homogenous materials. For example in Fig. 2(a) we present a mesh pair obtained by numerical optimization for

$$\varepsilon = \begin{pmatrix} 1 & \varepsilon_{xy}(x,y) \\ \varepsilon_{xy}(x,y) & 1 \end{pmatrix}, \quad \text{with} \quad \varepsilon_{xy}(x,y) = \begin{cases} \left(\frac{1}{2} - \frac{|y|}{l_y}\right) \sin\left(\frac{\pi}{l_x}\left(x + \frac{l_x}{2}\right)\right) & \text{if} \quad |x| \le \frac{l_x}{2} \\ 0 & \text{if} \quad |x| > \frac{l_x}{2} \end{cases}, \tag{60}$$

where $l_x$ and $l_y$ are lengths of the mesh in $x$ and $y$ direction, respectively. The mesh shown in Fig. 2(a) guarantees that the material matrix constructed is diagonal.

## 6. 3D CONSIDERATIONS

In 3D we first need to check when the set of conditions in Eq. (48) can be fulfilled by a mesh pair. For simplicity we assume that the material properties are constant $\xi = \text{const.}$ and therefore no averaging is needed, i.e., $\overline{\xi} = \xi$. We also assume that the material relations are given by (17) and (18) from which follows that the material mapping $\xi$ is self-conjugate, i.e., $\xi^\dagger = \xi$. A proportionality relation $\sim$ is defined as

$$a \sim b \Leftrightarrow a = \alpha b, \tag{61}$$

where $\alpha \in \mathbb{R}$ is the proportionality factor. As a possible constraint we consider an exemplary primal edge $l$ and its dual facet $\tilde{p}$, see Fig. 2(b). On the one hand, the mean orientation of the dual facet according to Eq. (48) should be proportional to

$$\tilde{p} \sim I\xi^{-1}(l). \tag{62}$$

On the other hand, it can be calculated from orientations of the dual edges $\tilde{l}_i$

$$\tilde{p} = \frac{1}{4}\left(\tilde{l}_1 \wedge \tilde{l}_2 + \tilde{l}_2 \wedge \tilde{l}_3 + \tilde{l}_3 \wedge \tilde{l}_4 + \tilde{l}_4 \wedge \tilde{l}_1\right). \tag{63}$$

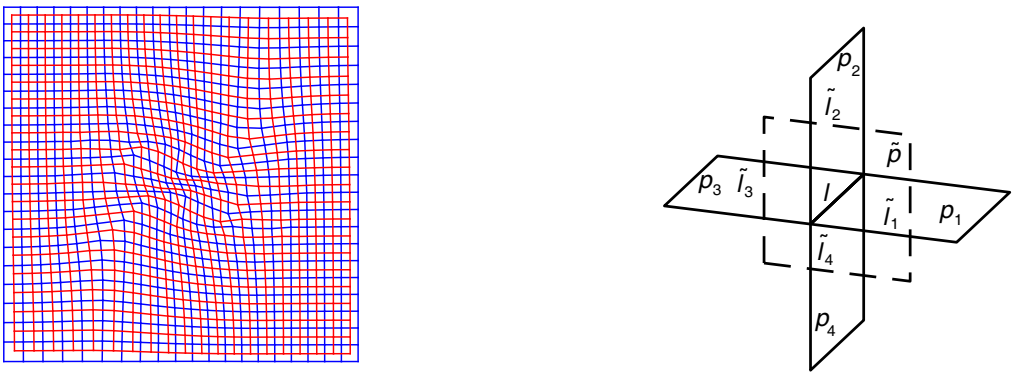


(a) The optimized mesh for continuous but not constant $\varepsilon(x, y)$. Blue lines represent the primal mesh and the red ones the dual one.

(b) Primal edge $l$ and its dual facet $\tilde{p}$. Depicted are also neighbouring facets $p_i$ and their dual edges $\tilde{l}_i$.

**Figure 2.** (a) Optimization mesh and (b) image visualizing the relation of primary edges and dual facets.

Let us suppose that the edge $l$ is one of the $x$-edges of the Cartesian grid. Since $\xi$ is constant it follows that $l_1 \sim l_3$ and $l_2 \sim l_4$. It simplifies the expression for the mean orientation

$$\tilde{p} \sim \tilde{l}_1 \wedge \tilde{l}_2, \tag{64}$$

where $\tilde{l}_1$ and $\tilde{l}_2$ according to (48) are proportional to

$$\tilde{l}_1 \sim I\xi^{-1}(p_1) = I\xi^{-1}(I\sigma_z) = -\mu_{za}\sigma_a \tag{65}$$

$$\tilde{l}_2 \sim I\xi^{-1}(p_2) = I\xi^{-1}(I\sigma_y) = -\mu_{ya}\sigma_a. \tag{66}$$

From which follows that the left-hand side of Eq. (62) is

$$\tilde{p} \sim \mu_{zb}\mu_{yc}\sigma_b \wedge \sigma_c. \tag{67}$$

Expanding right-hand side of Eq. (62) gives

$$\tilde{p} \sim I\xi^{-1}(l) = I\left[\varepsilon^{-1}\right]_{xa}\sigma_a. \tag{68}$$

Using the identity

$$\sigma_b \wedge \sigma_c = \epsilon_{abc} I\sigma_a, \tag{69}$$

where $\epsilon_{abc}$ is a permutation symbol: $\epsilon_{abc} = +1$ if $\{a, b, c\}$ is an even permutation of $\{1, 2, 3\}$, and $\epsilon_{abc} = -1$ if $\{a, b, c\}$ is an odd permutation of $\{1, 2, 3\}$. We obtain from Eq. (62)

$$I \left[\varepsilon^{-1}\right]_{xa} \sigma_a \sim \mu_{zb}\mu_{yc}\epsilon_{abc} I\sigma_a, \tag{70}$$

which simplifies to

$$\left[\varepsilon^{-1}\right]_{xa} = \alpha\mu_{zb}\mu_{yc}\epsilon_{abc} = -\alpha\nu_{xa}. \tag{71}$$

Repeating the same reasoning for $y$ and $z$ edges and using the symmetry of $\varepsilon$ and $\mu$ we arrive at the sufficient condition

$$\varepsilon = \alpha\mu, \tag{72}$$

which guarantees constructing the optimal primal/dual mesh pair. Please note that Eq. (72) states that $\varepsilon$ and $\mu$ must have not only the same main axes, but also the same eigenvalues associated with the main axes. The condition is not necessary. For example, in the case when the Cartesian grid axes are chosen as main axes of $\varepsilon$ and $\mu$, i.e., when $\varepsilon$ and $\mu$ are diagonal, the condition from above is relaxed, i.e., both $\varepsilon$ and $\mu$ may have arbitrary entries (eigenvalues) on their diagonals.

The condition in Eq. (72) has been derived for the Cartesian grid and flat facets of the dual mesh. One may wonder whether this result holds for other mesh pairs. From Eq. (48) it follows that

$$\left\langle \xi_j \left( I\widetilde{W}_j \right) W_j \right\rangle_2 = 0 \quad \text{and} \quad \left\langle \xi_j \left( I\widetilde{W}_j \right) W_j \right\rangle_4 = 0. \tag{73}$$

Noting that $\langle \xi_j (I\widetilde{W}_j) W_j \rangle_4$ is non-zero only for rather extraordinary and pathological choices of the primal/dual mesh, we require that only Eq. (73)-left is satisfied.

We explore Eq. (73)-left on a deformed FIT mesh, i.e., we allow primal and dual nodes to move while keeping the connectivity. In this case Eq. (73)-left is an overdetermined system of nonlinear equations whose variables are positions of the primal/dual nodes. We form a goal function

$$K = \sum_j \left\langle \xi_j \left( I\widetilde{W}_j \right) W_j \right\rangle_2^2 \tag{74}$$

and look for its minimum. According to our investigations if Eq. (72) is satisfied the obtained minimum is zero, i.e., all equations of the overdetermined system are simultaneously solved. Moreover, if Eq. (72) is violated then the obtained minimum is greater than zero showing that not all of Eq. (73)-left can be solved simultaneously. This is in agreement with our predictions derived in the case of Cartesian primal mesh. Since we have not found any counterexample, i.e., the mesh pair for which $K = 0$, and Eq. (72) is violated, we expect Eq. (72) to hold for arbitrary meshes and only relaxed if we use Cartesian grid with axes aligned to the main axes of $\varepsilon$ and $\mu$.

## 7. CONCLUSION

The classical orthogonal FIT mesh pair is a proper choice for scalar and diagonal material tensors. However, in the case of deformed primal grids, the orthogonal dual results in diagonal material matrices only for scalar material coefficients. When $\varepsilon$ is a tensor and non-diagonal entries in material matrix are disregarded, the convergence is lost. However, adapting the dual mesh according to our criterion fixes the problem and allows to treat arbitrary material tensor consistently. In 3D setting, we have shown that the permittivity tensor being proportional to the permeability tensor implies existence of the mesh pair guaranteeing diagonal material matrices. However, proportionality of material tensors is very restrictive for physical applications.

## ACKNOWLEDGMENT

The authors would like to thank Professor Stefan Kurz for fruitful discussions. The work of the first and second authors is supported by the 'Excellence Initiative' of the German Federal and State Governments and the Graduate School of CE at Technische Universitaet Darmstadt.

## REFERENCES


1. Doran, C. and A. Lasenby, *Geometric Algebra for Physicists*, 2nd Edition, Cambridge University Press, Cambridge, 2003.
2. Klimek, M., U. Roemer, S. Schoeps, and T. Weiland, "Space-time discretization of Maxwell's equations in the setting of geometric algebra," *IEEE Proceedings of 2013 URSI International Symposium on Electromagnetic Theory (EMTS)*, 1101–1104, 2013.
3. Tonti, E., "Finite formulation of the electromagnetic field," *Progress In Electromagnetics Research*, Vol. 32, 1–44, 2001.
4. Weiland, T., "Time domain electromagnetic field computation with finite difference methods," *International Journal of Numerical Modelling*, Vol. 9, 295–319, 1996.
5. Sobczyk, G., "Simplicial calculus with geometric algebra," *Clifford Algebras and Their Applications in Mathematical Physics*, 279–292, Springer, 2011.
6. Hestenes, D., "Differential forms in geometric calculus," *Clifford Algebras and their Applications in Mathematical Physics*, 269–285, Springer, 1993.
7. Mullen, P., P. Memari, F. de Goes, and M. Desbrun, "HOT: Hodge-optimized triangulations," *ACM Trans. Graph.* Vol. 30, 103:1–103:12, 2011.
8. Bellver-Cebreros, C. and M. Rodriguez-Danta, "An alternative model for wave propagation in anisotropic impedance-matched metamaterials," *Progress In Electromagnetics Research*, Vol. 141, 149–160, 2013.
9. Lindell, I. V., "Electromagnetic wave equation in differential-form representation," *Progress In Electromagnetics Research*, Vol. 54, 321–333, 2005.
10. Stern, A., Y. Tong, M. Desbrun, and J. E. Marsden, "Geometric computational electrodynamics with variational integrators and discrete differential forms," *Geometry, Mechanics, and Dynamics*, Vol. 73, 437–475, Springer, 2015.